Received: 5 October 2020 | Revised: 25 January 2021 | Accepted: 1 February 2021

IET Nanobiotechnology

DOI: 10.1049/nbt2.12045

The Institution of Engineering and Technology WILEY

REVIEW

A review on three-dimensional graphene: Synthesis, electronic and biotechnology applications-The Unknown Riddles

Pradheep Thiyagarajan

Department of Micro & Nano Electronics, School of Electronics Engineering (SENSE), Vellore Institute of Technology, Vellore, India

Correspondence

Pradheep Thiyagarajan, Department of Micro & Nano Electronics, School of Electronics Engineering (SENSE), Vellore Institute of Technology, Vellore 632014, India.
Email: pradheep.t@vit.ac.in

Abstract

In the last decade, carbon-based nanostructures such as buckyball (C_{60}), carbon nanotube (CNT), graphene and three-dimensional (3D) graphene have been identified as promising materials for electronic, electrochemical energy storage (batteries and supercapacitors), optical and sensing applications. Since the discovery of graphene in 2004, scientists have devised mass production techniques and explored graphene as a promising material for a wide range of applications. Most of the electronic and solar cell applications require materials with good electronic conductivity, mobility and finite bandgap. Graphene is a zero bandgap material which prevents it from the mainstream applications. On the other hand, 3D graphene has good electronic conductivity, mobility, bandgap and electrochemical properties. This review article will focus on the synthesis of the 3D graphene, its structure-property relationships, biotechnology and electronic applications and the hidden properties that are yet to be explored fully.

1 | INTRODUCTION

Carbon is one of the fascinating materials that provides the basis of life on the Earth [1]. It is widely employed for electronics [2], drug delivery [3], energy storage [4], solar cells [5], sensors [6] applications etc. Diamond and graphite are the common carbon allotropes which have sp^3 and sp^2 hybridised carbon atoms, respectively [7]. Diamond possesses insulator properties, whereas graphite has semi-conducting properties. Graphite is a three-dimensional (3D) structure of sp^2 hybridised carbon atoms, which has a higher electronic mobility and thermal conductivity than diamond. In 1985, scientists successfully reported on synthesising the 0D fullerene also called the buckyball structures comprising of sp^2 hybridised 60 carbon atoms named as C_{60} molecules [8]. C_{60} has a hollow carbon cage-like structure which has a predicted band gap of 0.7–2.5 eV based on various calculations and experiments [9]. Many studies have been conducted on exploring the possibility of using C_{60}, fullerene films [10] and fullerene composites for optical, electronic, medical and energy applications recently. C_{60} films have an electronic conductivity varying from 4×10^{-3} S/cm to 4×10^{-7} S/cm depending on the film thickness and a mobility of 0.08 cm^2/Vs [11]. Low electronic conductivity and mobility of the C_{60} films make them unsuitable for electronic applications. Composites of fullerene/metal oxide or fullerene finds application in drug delivery [12], solar cell [13] and other medical applications [14, 15]. Since their discovery of Carbon nanotubes (CNT) in 1991 [16], they have been studied for a wide range of applications like transistor [17], actuators [18], sensors [19], thermal management [20], supercapacitors [21], biological studies [22, 23] etc. CNT can be constructed in two forms, namely, the single-walled CNT (SWCNT) and the multi-walled (MWCNT), which can be synthesised by any of the following techniques such as laser ablation [24], arc discharge [25], chemical vapour deposition (CVD) [26], catalytic synthesis [27], vapour liquid solid(VLS) growth [28, 29] etc. SWCNT is a single sheet of graphene rolled into a cylinder-like structure. The diameter of the SWCNT determines the band gap for instance 0.2–0.8 eV for 1–4 nm diameter nanotubes and mobility of $\sim 10^4$ cm^2/Vs at room temperature [30]. The electronic conductivity of the SWCNT is found to be between 10^4–10^5 S/cm and in case of CNT papers the conductivity is 10^3 S/cm [31], whereas the thermal conductivity of CNT is found to be ~2000 W/mK [32]. CVD is a mass production technique used to synthesise CNT but it produces CNT with both metallic and semi-conducting properties. It was a hard task to segregate the metallic and semi-conducting nanowires that will be used further for fabrication of devices. CNTs and their composites

are extensively used for fabrication of transistors, making memory devices [33], as current collector in solar cell [34], photo detectors [35], supercapacitors [36], batteries [37], fuel cells [38], biosensors [39] etc. The high thermal conductivity of the CNT reduces the prospect of replacing the channel material in the field effect transistor (FET) fabrication.

Since its synthesis in 2004 graphene, a 2D sheet of carbon atoms has been a game-changer in the various fields. Graphene can be synthesised by different methods such as scotch-tape method [40], chemical synthesis [41], CVD [42] etc. CVD has been a versatile technique for mass production of single-, bi- and few-layered graphene sheets. The single layer graphene (SLG) has more superior electronic, thermal properties than the bi-layer or the few-layer graphene (FLG). SLG has zero bandgap, ballistic electron transport, large catalytic activity sites, very high mobility (200,000 cm^2/Vs) at low temperature [43] for suspended graphene and high mobility at room temperature (10^3 cm^2/Vs) and very high thermal conductivity of ~3000 W/mK. A proof of concept graphene FET devices has been demonstrated in 2009 by the IBM scientists which was operating in the GHz frequency regime [44]. However, integration of a number of graphene FET in practical application will lead to excessive heating owing to its high thermal conductivity and zero bandgap of graphene would hinder the performance since performance tuning of circuits using band gap is not possible with graphene.

3D graphene-based structures that are different from graphite are synthesised via several techniques such as growing graphene on foam-like structures through CVD [45] solution synthesis of 3D graphene [46], template-assisted solution growth [47] etc. To analyse the number of graphene layers or defects, Raman spectroscopy has been evolved as an important tool. Raman spectroscopy is a powerful tool to study the clustering of sp^2 phase, disorders, number of graphene layers, presence of sp^2–sp^3 phase [48]. All the sp^2 hybridised carbon materials analysed through Raman spectroscopy will have a G-band peak ~1580 cm^{-1}. The D and G′ or 2D peak of Raman spectra provide information on electronic property and geometrical information. The disorder induced D peak in sp^2 hybridised carbon materials will be ~1350 cm^{-1}. The G′ or 2D peak is exclusive to grapheme-based materials that happens due to the double resonance process. The G′ or 2D peak will appear in the range of 2600–2800 cm^{-1} along with the G peak [49]. A pictorial representation of the Raman spectrum of the carbon materials is given in Figure 1.

The ratio of D to G peak is an important parameter in studying CNT and graphene in terms of defects. The ratio of 2D peak to G peak provides quantitative information about the number of graphene layers. 3D graphene foams should possess a good 2D/G peak ratio to have better electronic properties. There are many reviews available on 2D materials and their applications. Nevertheless, there has been limited review articles on 3D graphene-based materials for a specific application. This review article will try to bridge the gap and address the use of 3D graphene foams for biotechnology, sodium ion batteries, supercapacitors etc. In the next section, we will have a brief overview of the synthesis method of 3D graphene.

In terms of porous graphene-based films, they can be broadly classified into (i) homogenous porous graphene called Holey graphene [50] and (ii) heterogeneous porous graphene called 3D graphene foams [51]. The pores are further categorised into mesoporous (pore size: 2–50 nm), microporous (<2 nm pore size) and macroporous which have pore size > 50 nm. Holey graphene (HG) has a 2D structure with mesoporous pores and it is found to be suitable for electrochemical [52] and water-splitting applications [53]. The synthesis process of the HG has been standardized and research is progressing to improve its inherent material properties [53]. For supercapacitor and battery applications, graphene which has microporous and mesoporous pores is better suited [54]. For thermoelectric and biological applications, a combination of mesoporous and macroporous graphene is best suited. However, the synthesis of the mesoporous and macroporous graphene is a challenging task [55]. In addition, the size of the 3D graphene foam/mesoporous graphene film determines the structural and mechanical properties [56]. This article focuses on synthesis of homogenous and heterogeneous 3D graphene foams which have mesoporous and macroporous structures and their explored and unexplored properties.

2 | SYNTHESIS TECHNIQUES

The fabrication of 3D graphene foams has many advantages such as band gap opening, large surface area, better catalytic activity, low thermal conductivity and downside moderate electronic conductivity and mobility in comparison with graphene. The synthesis method used to fabricate 3D graphene foams dictates the above-mentioned properties. The synthesis methods can be broadly classified into two categories (i) template-assisted method and (ii) template-free method [57].

2.1 | Template-assisted growth of 3D graphene foams

CVD has been a reliable method for making the 3D graphene using nickel foams as a template using gaseous precursors at 1000°C under inert conditions as shown in Figure 2. The nickel foams have a pore size greater than 200 μm [45]. Hence, the removal of nickel foam after synthesis would lead to a structural collapse which can be prevented by coating a polymer layer on top of the graphene layer. The coating of polymer will lead to problems in etching, low catalytic activity. The 3D graphene synthesised by this method has light weight, good electrical conductivity and mobility and flexibility that is employed for supercapacitor applications [58].

The bandgap and band structure of the 3D graphene/Ni foam has been unexplored till date. Lee et al. synthesised 3D graphene foam (3D-NFG) by coating the substrate with PVA/$NiCl_2{\cdot}6H_2O$ precursor and pyrolysing them at 1000°C under inert conditions. The self-standing 3D graphene foams are

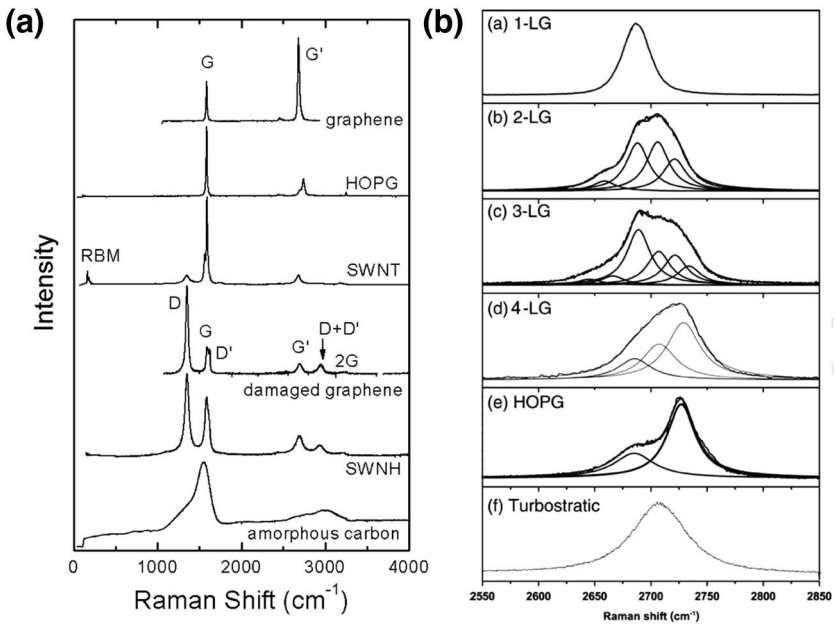

FIGURE 1 (a) Raman spectra from different types of sp^2 nanocarbons. The graphene-related structures are labelled next to their respective spectra. The main features (RBM and disorder-induced D, D′ and D + D′ bands; first-order Raman-allowed G band; and second-order Raman overtones G′ (2iTO) and 2G) are labelled in some spectra but the assignment applies to all of them. A detailed analysis of the frequency, line shape and intensity for these features gives a great deal of information about each respective sp^2 carbon structure. (b) The G′ spectra for graphene as a function of the number of layers [49] has been reproduced with permission from [49] 2010, American Chemical Society

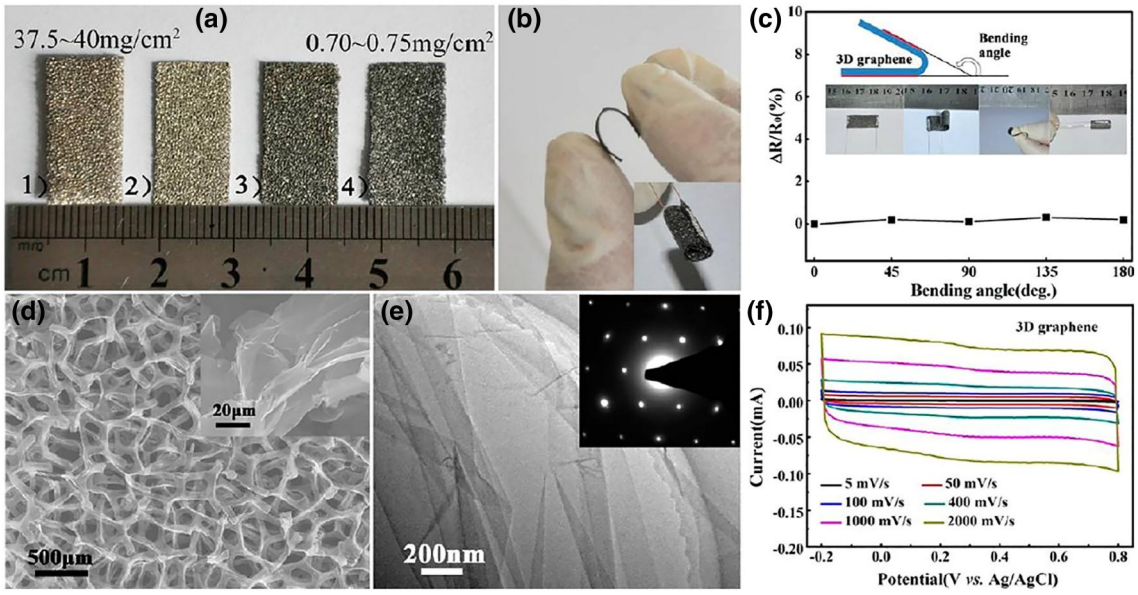

FIGURE 2 (a) Digital photographs of Ni foams with (1) and without (2) pressed and graphene-coated Ni foams before (3) and after (4) removal of the Ni networks. (b) Digital photograph of a free-standing and flexible 3D graphene network prepared from pressed Ni foam. Inset shows the curled 3D graphene networks. (c) Electrical-resistance variation of 3D graphene networks versus the different bending angles. Inset shows the digital photographs of different bending shapes. (d) SEM image of the 3D graphene networks after the removal of Ni foam. Inset shows high-magnification SEM image. (e) TEM image of a graphene sheet. Inset shows a SAED pattern of the corresponding GNS. (f) CVs of the 3D graphene network electrode in 0.5 M aqueous Na_2SO_4 electrolyte at different scan rates. Reproduced with permissions from [58] 2012, American Chemical Society

made by etching the nickel particles. The pore size of the 3D graphene varied between 40 and 100 nm with a much enhanced surface area that is suitable for electrolyte-based energy conversion and storage applications [59]. AAO template-based synthesis of 3D graphene has been tried to synthesise nanoporous 3D graphene with pore size around 60 nm [60]. The process and quality of the graphene synthesised on AAO template has been pictorially represented in Figure 3.

The AAO template-based synthesis of the graphene has the lowest electrical conductivity (10^{-3} S/cm) than 3D-NFG (10^3 S/cm) and 3D graphene on nickel foam (10^3–10^4 S/cm). Recently, many scientists have made composites such as MnO_2/3D graphene [58], NiO/3D graphene/Ni foam [62], $Ni(OH)_2$ nanoflakes/3D graphene/Ni foam [63], S, N co-doped graphene/Ni foam [64] testing their electrochemical performance. A detailed discussion of the applications and issues will be presented in section 3.

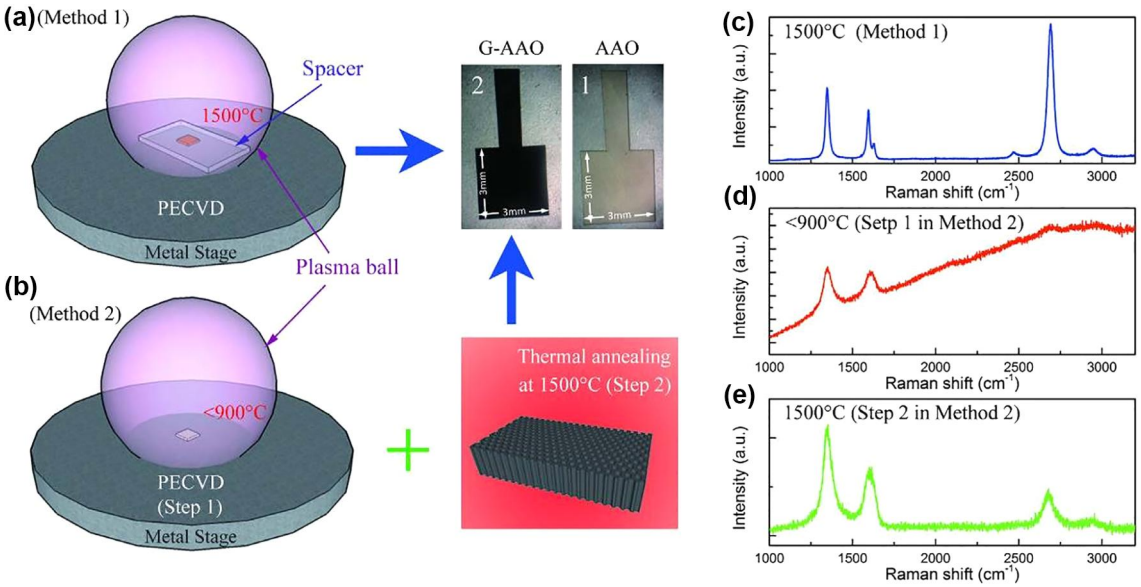

FIGURE 3 Fabrication processes and Raman spectra of 3D graphene and a-C on AAO. (a) Schematics of the one-step graphene fabrication method by PECVD process with the spacer in between the sample and the stage. (b) Schematics of the two-step method where the first step is the PECVD process without the spacer and the second step is thermal annealing of the a-C-AAO sample (produced by step 1) in vacuum at 1500°C using an electron beam. (c) An AAO sample before (1) and after (2) the fabrication process. (d)–(f) Raman spectra of graphene coated AAO (G-AAO by method 1), diamond-like carbon-coated AAO (a-C-AAO by the first step in method 2) and thermal annealed a-C-AAO (by the second step in method 2), respectively. Reproduced with permissions from [61] 2016 Spring Nature

2.2 | Template-assisted synthesis of 3D graphene powder

Silica/polystyrene (PS)/polymethyl methacrylate (PMMA) can be used as a template for 3D graphene growth which determines the pore size in the synthesised 3D graphene. Firstly, the silica/PS ball will be functionalised using metal precursor and using gaseous precursor as carbon source/metal and carbon precursor solution coated and pyrolysed/graphene oxide solution coated and heated at high temperatures to yield nanoporous 3D graphene powder after removing the metals [60] as shown in Figure 4. The 3D graphene powder has certain advantages such as large surface area and good catalytic activity due to the nanopores for the desalination purpose but they do suffer from low mobility and need the binder material to be attached to any substrate for device applications. 3D graphene foam can be synthesised by this process by coating the solution of silica/metal-carbon precursor on substrate and then heating it at high temperature (800–1000°C under inert conditions). The 3D graphene synthesised by these methods is known by different names such as 3D graphene balls, mesoporous graphene, chemically modified graphene etc. A schematic diagram of this process is provided below:

The MGB possesses a pore size of 4.27 nm, surface area of 508 m^2/g, electrical conductivity of 6.5 S/cm and specific capacitance of 206 F/g for supercapacitor applications. Choi et al. have synthesised 3D graphene using PS ball of 2 μm diameter as sacrificial templates and coated them with chemically modified grapheme.

2.3 | Solution-based synthesis of 3D graphene foams/films

The hydrothermal method is one of the solution techniques widely used to synthesise the metal oxide nanowire and nanostructures. Xu et al. [65] reported the self-assembly of the graphene hydrogel (SGH)-based structures by heating the uniform GO dispersion in an autoclave at 180°C for 24 h. Owing to the pressure exerted in the reaction, Π-Π stacking happens in the GO sheets, which leads to the 3D structure of the graphene. The morphology of the product can be varied by altering the GO concentration, reaction time and catalysers involved. This method is also applicable to synthesise nanocomposite of nanowire/3D graphene or nanoparticles/3D graphene or N-doped 3D graphene etc. The electrical conductivity of the SGH was found to be 5×10^{-3} S/cm [65]. Similarly, reduced graphene oxide films synthesised using new techniques yielded record high conductivity of nearly 6300 S/cm [66]. The Ag/rGO composites are reported to have conductivities of 2×10^3 S/m [67]. The hydrothermal method can be combined with the electrodeposition for making composite materials. The advantage of hydrothermal method is (i) low-a cost (ii) novel nanostructures can be formed, whereas the disadvantages are (iii) low electronic conductivity and (iv) hard to control the uniformity in the structures.

Electrodeposition is a cheap, non-toxic, low temperature technique that does not need the use of a binder for making electrodes and avoids the transfer procedure which will be beneficial for the structure. Graphene oxide solution can be electrodeposited on the Ni foam at a potential of −1 to 0 V at a

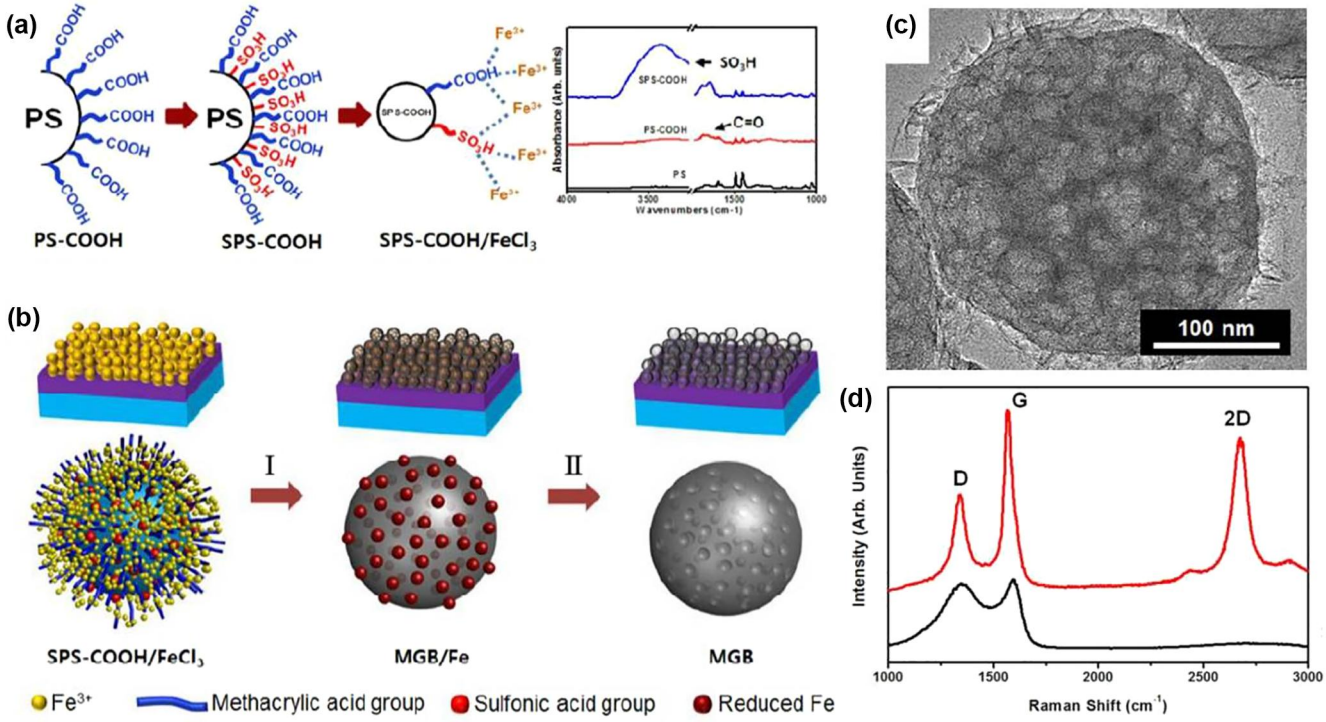

FIGURE 4 Schematic illustration of the mesoporous graphene nano-ball (MGB): (a) The fabrication process of SPS-COOH (functionalisation of PS via carboxylation and sulfonation) and the FT-IR spectra of the samples. (b) The fabrication process of MGB: step 1. Drop casting of the SPS-COOH/$FeCl_3$ solution onto the substrate and subsequent CVD growth of grapheme: step 2. The removal of iron domains to leave the MGB. (c) TEM of the MGB and (d) Raman spectra of SPS-COOH/$FeCl_3$ before (lower) and after (upper, MGB) CVD growth of graphene. Reproduced with permissions from ACS Nano 2013, 7, 7, 6047–6055

constant current of 1 mA for 300 s. It leads to the formation of the 3D graphene oxide structures on Ni foam substrate. A further annealing step in a reduction atmosphere will lead to the formation of the 3D graphene/Ni foam [68, 68]. This process is advantageous especially for the supercapacitor application, the reason being that phosphide or metal oxide materials can be easily coated on top of the 3D graphene/Ni foam structures without the use of any binder material.

Ice-segregation induced self-assembly (ISISA) [69] is a process by which amphiphilic polymers and carbon sources will be frozen in liquid nitrogen to form a variety of structures. Chitosan and graphene oxide or polystyrene sulfonate (PSS) stabilised graphene oxide or poly vinyl alcohol (PVA) and graphene oxide (GO) are freeze-dried to make 3D graphene structures. In this process, the amphiphilic material acts as a template for the growth. There are various experimental parameters such as the concentration of GO, freezing rate, freezing direction etc. A cyro-processing step is done for the reduction of the graphene oxide followed by an annealing process at 200°C. The 3D graphene synthesised by this method has a lamellar structure and pore diameter varying between 5 and 50 μm. The pictorial schematic and morphological characteristics of 3D graphene synthesised using CHI has been presented in Figure 5 and Figure 6.

The mobility of the ISISA synthesised 3D graphene is very low and hence it cannot be used for electronic applications. The ISISA synthesised 3D graphene is employed for biological applications, fuel cell etc.

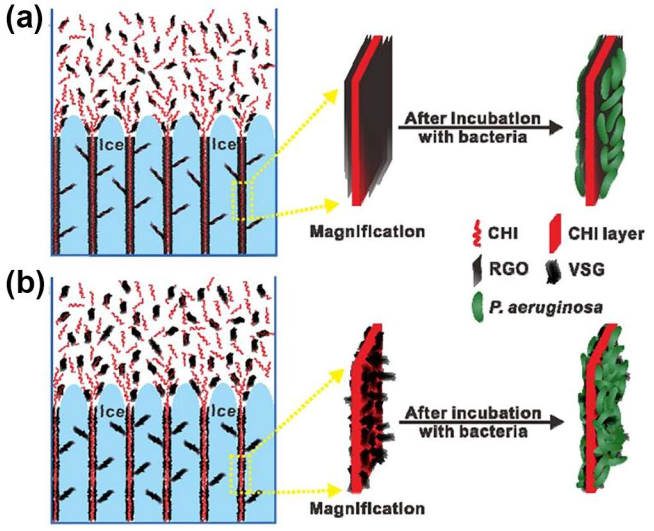

FIGURE 5 Schematic illustration of the layered and branched structure formation process of CHI/RGO (a) and CHI/VSG (b) Scaffolds and their contact with bacteria. Reproduced with permission from [70] 2012, American Chemical Society

In the previously reported studies on 3D graphene synthesised by various methods; electronic conductivity and mobility have been studied, whereas the electronic band structure and band gap have not been studied so far. Angle resolved photo emission spectroscopy (ARPES) would be a

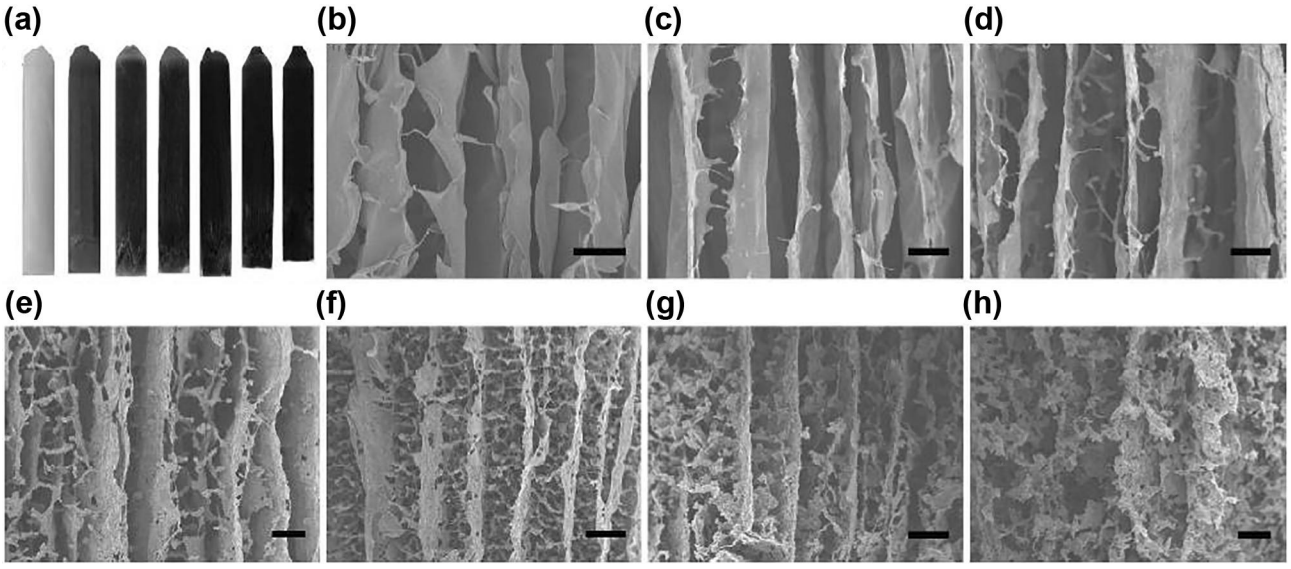

FIGURE 6 The photograph of all CHI/VSG scaffolds (a). The SEM images of CHI (b), CHI/VSG-5 (c), CHI/VSG-10 (d), CHI/VSG-30 (e), CHI/VSG-50 (f), CHI/VSG-60 (g), and CHI/VSG-70 (h) scaffolds. The scale bars are 50 μm. Reproduced with permission from [70] 2012, American Chemical Society

suitable technique to unravel the band structure of 3D graphene. Based on the band structure revelations, the electronic properties with regard to pore size relation can be derived. Secondly, in the 3D graphene there is not a straight forward approach in choosing nano-sized pores or micron-sized pores. The application and the property requirements dictates the pore size, which, in turn affect the surface area, electrical and thermal conductivity. Thirdly, the magnetic properties of 3D graphene hasn't been extensively studied as graphene. In the next section, we will see the various applications of 3D graphene, their issues and solutions.

3 | APPLICATIONS

Holey graphene is a modified graphene nanosheet with homogenized nanosized pores in it. Therefore, holey graphene has a band gap without much of compromising electrical conductivity and other properties of graphene [53]. Holey graphene does outperform graphene in some applications such as supercapacitors [50], batteries [71], water desalination [72], bioseparation, fuel cell [73], hydrogen storage [74] etc. The 3D graphene/3D graphene composites do have a band gap and outshine the holey graphene in terms of performance in certain application. Since the band gap of the 3D graphene hasn't been studied and mobility is limited, they aren't used for transistor applications. This section is subcategorised into four sub-sections namely (i) supercapacitor applications (ii) Batteries (iii) energy conversion applications and (iv) biological applications of 3D graphene.

3.1 | Supercapacitor applications

Supercapacitors have been gaining attention due to their high power density, fast charging-discharging, lightweight and cheapness. Electric double layer capacitance (EDLC) and pseudo capacitor are two categories of supercapacitors. Since the discovery of 3D graphene it has been used for supercapacitor application. For comparing the electrochemical charge storage mechanism several factors, such as area of the film/mass loading, surface area, pore size, scan rate, electrolyte, electrolyte concentration, capacity retention should be considered. A detailed review of synthesis and application of holey graphene has been reported in the previous literatures [36, 60]. Holey graphene has the highest surface area of 1874 m^2/g, pore size of 3.2 nm and specific capacitance of 268 F/g [72]. The 3D graphene (MGB), synthesised as a powder, has been examined for the supercapacitor displaying a surface area of 508 m^2/g, pore size of 4.7 nm and specific capacitance of 206 F/g and electrical conductivity of 6.5 S/cm [46].

3.2 | Batteries

Batteries have high energy density and less power density than supercapacitors. Lithium ion (Li-ion) batteries have been dominating the market for the last 2 decades varying from portable applications to electric vehicles. However, the energy density required for electric vehicle is insufficient when powered by Li-ion batteries. Metal-air batteries are new kind of batteries where the air cathode material is the carbon and the binder and anode material can be a pure metal with theoretical energy density as high as 12,000 Wh/Kg and practical energy density is 4000 Wh/Kg for Li-air batteries. Among the different metal-air (Li-air, Zinc-air, Aluminium-air, sodium-air) batteries Li-air batteries have high energy density. There are four different configurations of Li-air batteries and a detailed explanation of the structure and performance factors are mentioned in this literature [75]. Graphene/graphene composites/3D graphene are alternative materials to the air cathode material as they possess greater

number of catalytic active sites. Nitrogen-doped graphene and graphene composites, such as perovskite oxide/nitrogen-doped graphene [76], α-MnO_2 on graphene-coated carbon microfibers [77], polystyrene sulfonate/graphene and Mn_3O_4/graphene [78], have been suggested as an alternative air cathode material as they possess increased catalytic activity thereby boosting the energy density of the system.

3.3 | Energy conversion

Thermoelectric energy conversion is one of the methods to convert waste heat into electricity utilising efficient materials. Thermoelectric properties are measured by means of the thermoelectric figure of merit (ZT), given by $ZT = S^2\sigma/KT$, where S is the Seebeck coefficient, σ is the electrical conductivity, K is the thermal conductivity and T is the temperature. For a commercially efficient thermoelectric material, the ZT should be 3 or more. An ideal thermoelectric material should possess the electrical conductivity of the metal, Seebeck coefficient of insulator and thermal conductivity of semiconductor material. Hence, scientists have been trying hard for the last 6 decades to make materials that match the property of an ideal material. With respect to graphene, it has been found to have a high thermal and electrical conductivity and moderate Seebeck coefficient, which lead to low ZT values [79]. The 3D graphene has a high Seebeck coefficient, low thermal conductivity (2 orders of magnitude lower than graphene's thermal conductivity) and moderate electrical conductivity to attain a reasonable ZT value. The reason for the performance enhancement in 3D graphene is due to the (i) band-gap opening which leads to mini band formation (ii) roughness of the film and (iii) pore size which play a crucial role of uninterrupted electron transport, interrupting the phonon transport. 3D grapheme-based composites such as bismuth-3D graphene composites. The niobium-3D graphene composite can be the next possible choice of plausible ideal materials for thermoelectric applications. Recently, piezoelectric and triboelectric energy conversion is gaining attention for powering smart wearable devices. Graphene is a promising material for this application because of its inherent lightweight, flexible and electrically conductive nature. Graphene [80] and graphene/PVDF [81] composites are being extensively reported to generate mill-watt power for this mechanical to electrical energy conversion applications.

3.4 | Biotechnology applications

Carbon materials are mostly used in biological applications such as biomarkers [82], biosensors [83], drug delivery [84], bio

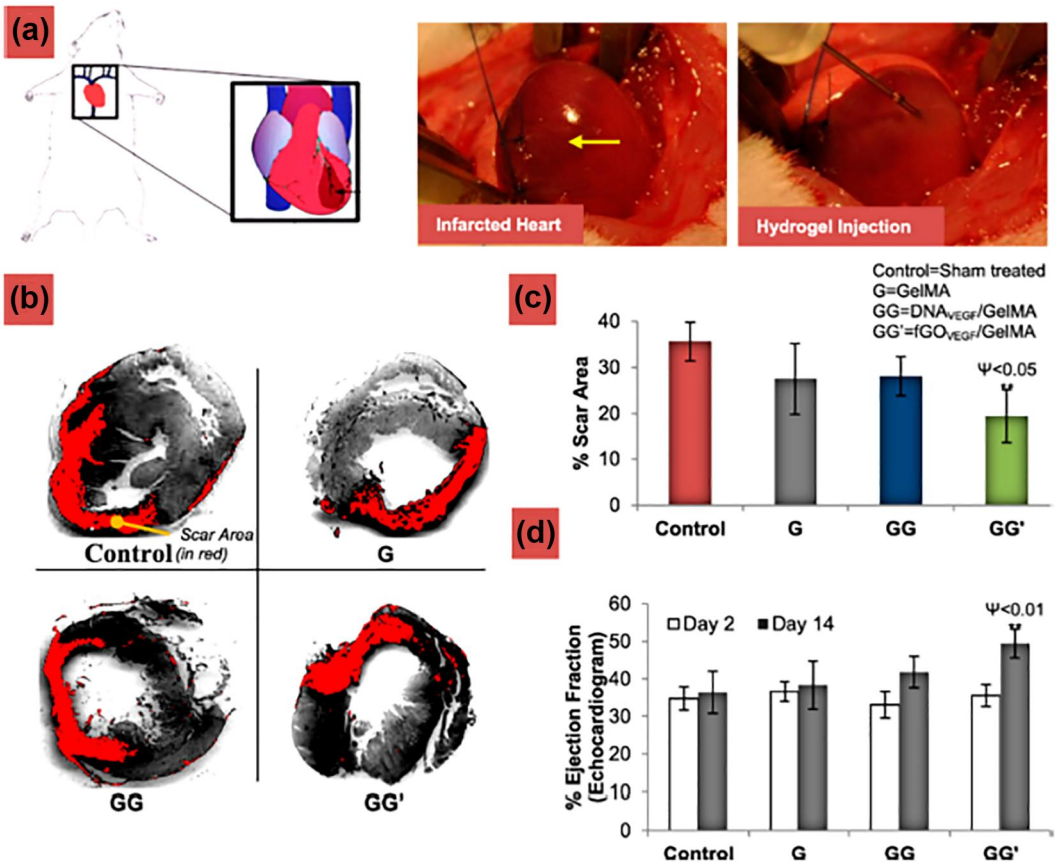

FIGURE 7 (A) Schematic image of the rat's heart with acute myocardial infarction (AMI). (B and C) Determination of the scar area by morphometric analysis. GG' (fGO/DNAVEGF/GelMA), GG (GelMA with free pDNAVEGF), G (only GelMA), and control (non-treated). (D) Echocardiographic assessment of cardiac function. Reproduced with permission from ref [89] 2017 copyright American Chemical Society

functionalisation [83] etc. Bio functionalisation of graphene/3D graphene has been done using peptide and cellulose as well as other biomolecules to sense/detect living cells/tumour cells/cancer cells. The reasons for using carbon materials are they are cheap, biocompatible, biodegradable, harmless to human and environment. Electrochemical sensing and plasmonic/FRET-based sensing are two of the major sensing mechanisms for bio sensors. Since graphene is a semi-metal, it possesses good plasmonic properties and the high thermal conductivity makes it a bit tough to sense the cancer cells based on temperature. A detailed review on bio functionalisation and bio sensing of graphene is presented in this literature [85]. Since 3D graphene has low thermal conductivity and electrochemically active, it is a promising alternative to grapheme-based materials for the biotechnology applications.

In the last decade, there were several works on deploying graphene for bio electrochemical sensing [86, 87]. However, the 3D graphene has more surface area than its 2D counterparts due to which more enzymes and catalytic activity will interact with the material surface. The 3D graphene is preferred as an electrode material for microbial/acidic fuel cells. There has been a wide range of reported studies on structure-property relationship in 3D graphene for biological fuel cells.

Functional 3D-graphene-based nanomaterial (3D rGO, 3D graphene, graphene-based aerogel/hydrogel, 3D graphene composites) were used as biocompatible materials for tissue and bone regeneration applications [88]. The biological performance results of 3D graphene composites checked on rat heart are given in Figure 7.

The 3D graphene materials, along with peptide structures, are an efficient self-adjustable material, possessing biomimic structures used for regeneration applications. In addition, these materials are also used for toxicity studies [90], pathogen detection [91], biomedical implants [92] etc.

4 | CONCLUSION AND FUTURE DIRECTIONS

This article provided an overview about various carbon nanostructures including the CNT, graphene, holey graphene and 3D graphene foam. The synthesis method is briefly discussed for well-known CNT and graphene, and the 3D graphene synthesis is discussed in detail. In the 3D-graphene-based structure, the variation of the pore size causes a considerable change in the properties for supercapacitor, thermoelectric and biotechnology applications. The pathways to improve the properties of the 3D graphene for various applications are outlined in this article. To mention an important one, the band structure of the 3D graphene synthesised by various methods needs to be carefully studied. The 3D graphene-based composites have to be explored in detail for biotechnology and thermoelectric applications.

CONFLICT OF INTEREST

There is no conflict of interest.

DATA AVAILABILITY STATEMENT

Data subject to third-party restrictions. The figures from reference papers were used with copyright permissions from publishers like ACS, RSC, Nature etc. The copyright permissions are highlighted in the article as per the guidelines.

ORCID

Pradheep Thiyagarajan https://orcid.org/0000-0003-1477-7673

REFERENCES

1. Hirsch, A.: The era of carbon allotropes. Nat. Mater. 9(11), 868–71 (2010)
2. Shi, E., et al.: Carbon nanotube network embroidered graphene films for monolithic all-carbon electronics. Adv. Mater. 27(4), 682–688 (2015)
3. Wong, B.S., et al.: Carbon nanotubes for delivery of small molecule drugs. Adv. Drug Deliv. Rev. 65(15), 1964–2015 (2013)
4. Pandolfo, A.G., Hollenkamp, A.F.: Carbon properties and their role in supercapacitors. J. Power Sources. 157(1), 11–27 (2006)
5. Wu, M., et al.: Low-cost dye-sensitised solar cell based on nine kinds of carbon counter electrodes. Energy Environ. Sci. 4(6), 2308–2315 (2011)
6. Yamada, T., et al.: A stretchable carbon nanotube strain sensor for human-motion detection. Nat. Nanotechnol. 6(5), 296–301 (2011)
7. Falcao, E.H., Wudl, F.: Carbon allotropes: beyond graphite and diamond. J. Chem. Technol. Biotechnol. 82(6), 524–531 (2007)
8. Kroto, H.W., et al.: C60: Buckminsterfullerene. Nature. 318(6042), 162–163 (1985)
9. Lof, R.W., et al.: Band gap, excitons, and Coulomb interaction in solid C 60. Phys Rev Lett. 68(26), 3924–3927 (1992)
10. Hebard, A.F., et al.: Deposition and characterisation of fullerene films. Appl. Phys. Lett. 59(17), 2109–2111 (1991)
11. Haddon, R.C., et al.: C60 thin film transistors. Appl. Phys. Lett. 67(1), 121–123 (1995)
12. Afreen, S., et al.: Functionalised fullerene (C60) as a potential nanomediator in the fabrication of highly sensitive biosensors. Biosens Bioelectron. 63, 354–364 (2015)
13. Graetzel, M., et al.: Materials interface engineering for solution-processed photovoltaics. Nature. 488(7411), 304–312 (2012)
14. Vandrovcova, M., et al.: Fullerene C60 and hybrid C60/Ti films as substrates for adhesion and growth of bone cells. Phys. Status Solidi A. 205(9), 2252–2261 (2008)
15. Sutradhar, S., Patnaik, A.: A new fullerene-C60–nanogold composite for non-enzymatic glucose sensing. Sensor Actuat. B Chem. 241, 681–689 (2017)
16. Iijima, S.: Helical microtubules of graphitic carbon. Nature. 354(6348), 56–58 (1991)
17. Javey, A., et al.: Ballistic carbon nanotube field-effect transistors. Nature. 424(6949), 654–657 (2003)
18. Baughman, R.H., et al.: Carbon nanotube actuators. Science. 284(5418), 1340–1344 (1999)
19. Ghosh, S., Sood, A.K., Kumar, N.: Carbon nanotube flow sensors. Science. 299(5609), 1042–1044 (2003)
20. Biercuk, M.J., et al.: Carbon nanotube composites for thermal management. Appl. Phys. Lett. 80(15), 2767–2769 (2002)
21. An, K.H., et al.: Supercapacitors using single-walled carbon nanotube electrodes. Adv. Mater. 13(7), 497–500 (2001)
22. Singh, R., et al.: Tissue biodistribution and blood clearance rates of intravenously administered carbon nanotube radiotracers. Proc. Natl. Acad. Sci. U.S.A. 103(9), 3357–3362 (2006)
23. Liu, Z., et al.: Preparation of carbon nanotube bioconjugates for biomedical applications. Nat. Protoc. 4(9), 1372–1381 (2009)
24. Zhang, Y., Iijima, S.: Microscopic structure of as-grown single-wall carbon nanotubes by laser ablation. Philos. Mag. Lett. 78(2), 139–144 (1998)
25. Stephan, O., et al.: Doping graphitic and carbon nanotube structures with boron and nitrogen. Science. 266(5191), 1683–1685 (1994)

26. Yudasaka, M., et al.: Specific conditions for Ni catalysed carbon nanotube growth by chemical vapour deposition. Appl. Phys. Lett. 67(17), 2477–2479 (1995)
27. Kiang, C.-H., et al.: Catalytic synthesis of single-layer carbon nanotubes with a wide range of diameters. J. Phys. Chem. 98(26), 6612–6618 (1994)
28. Kukovitsky, E.F., L'Vov, S.G., Sainov, N.A.: VLS-growth of carbon nanotubes from the vapour. Chem. Phys. Lett. 317(1), 65–70 (2000)
29. Prasek, J., et al.: Methods for carbon nanotubes synthesis—review. J. Mater. Chem. 21(40), 15872–15884 (2011)
30. Zhao, Y., Liao, A., Pop, E.: Multiband mobility in semiconducting carbon nanotubes. IEEE Electron. Device Lett. 30(10), 1078–1080 (2009)
31. Zhao, W., et al.: Flexible carbon nanotube papers with improved thermoelectric properties. Energy Environ. Sci. 5(1), 5364–5369 (2012)
32. Lindsay, L., Broido, D.A., Mingo, N.: Diameter dependence of carbon nanotube thermal conductivity and extension to the graphene limit. Phys. Rev. B. 82(16), 161402 (2010)
33. Choi, W.B., et al.: Carbon-nanotube-based nonvolatile memory with oxide–nitride–oxide film and nanoscale channel. Appl. Phys. Lett. 82(2), 275–277 (2003)
34. Ulbricht, R., et al.: Transparent carbon nanotube sheets as 3-D charge collectors in organic solar cells. Sol Energy Mater. Sol. Cell. 91(5), 416–419 (2007)
35. Arnold, M.S., et al.: Broad spectral response using carbon nanotube/organic semiconductor/C60 photodetectors. Nano. Lett. 9(9), 3354–3358 (2009)
36. Chen, Z., et al.: High-performance supercapacitors based on intertwined CNT/V2O5 nanowire nanocomposites. Adv. Mater. 23(6), 791–795 (2011)
37. Wang, J.-Z., et al.: Development of MoS2–CNT composite thin film from layered MoS2 for lithium batteries. Adv. Energy Mater. 3(6), 798–805 (2013)
38. Huang, J., et al.: Nickel oxide and carbon nanotube composite (NiO/CNT) as a novel cathode non-precious metal catalyst in microbial fuel cells. Biosens. Bioelectron. 72, 332–339 (2015)
39. Wang, J.: Carbon-nanotube based electrochemical biosensors: a review. Electroanalysis. 17(1), 7–14 (2005)
40. Novoselov, K.S., et al.: Electric field effect in atomically thin carbon films. Science. 306(5696), 666–669 (2004)
41. Chen, L., et al.: From nanographene and graphene nanoribbons to graphene sheets: chemical synthesis. Angew. Chem. Int. Ed. 51(31), 7640–7654 (2012)
42. Bae, S., et al.: Roll-to-roll production of 30-inch graphene films for transparent electrodes. Nat. Nanotechnol. 5(8), 574–578 (2010)
43. Du, X., et al.: Approaching ballistic transport in suspended graphene. Nat. Nanotechnol. 3(8), 491–495 (2008)
44. Lin, Y.-M., et al.: Operation of graphene transistors at gigahertz frequencies. Nano. Lett. 9(1), 422–426 (2009)
45. Chen, Z., et al.: Three-dimensional flexible and conductive interconnected graphene networks grown by chemical vapour deposition. Nat. Mater. 10(6), 424–428 (2011)
46. Lee, J.-S., et al.: Chemical vapour deposition of mesoporous graphene nanoballs for supercapacitor. ACS Nano. 7(7), 6047–6055 (2013)
47. Yoon, J.-C., et al.: Three-dimensional graphene nano-networks with high quality and mass production capability via precursor-assisted chemical vapour deposition. Sci. Rep. 3(1), 1788 (2013)
48. Ferrari, A.C., et al.: Raman spectrum of graphene and graphene layers. Phys. Rev. Lett. 97(18), 187401 (2006)
49. Dresselhaus, M.S., et al.: Perspectives on carbon nanotubes and graphene Raman spectroscopy. Nano. Lett. 10(3), 751–758 (2010)
50. Xu, Y., et al.: Holey graphene frameworks for highly efficient capacitive energy storage. Nat. Commun. 5(1), 4554 (2014)
51. Jiang, L., Fan, Z.: Design of advanced porous graphene materials: from graphene nanomesh to 3D architectures. Nanoscale. 6(4), 1922–1945 (2014)
52. Lin, Y., et al.: Holey graphene nanomanufacturing: structure, composition, and electrochemical properties. Adv. Funct. Mater. 25(19), 2920–2927 (2015)
53. Lokhande, A.C., et al.: Holey graphene: an emerging versatile material. J. Mater. Chem. 8(3), 918–977 (2020)
54. Qu, J., et al.: Dense 3D graphene macroforms with nanotuned pore sizes for high performance supercapacitor electrodes. J. Phys. Chem. C. 119(43), 24373–24380 (2015)
55. Yang, T., et al.: Tailoring pores in graphene-based materials: from generation to applications. J. Mater. Chem. 5(32), 16537–16558 (2017)
56. Shen, Z., et al.: Size of graphene sheets determines the structural and mechanical properties of 3D graphene foams. Nanotechnology. 29(10), 104001 (2018)
57. Qiu, B., Xing, M., Zhang, J.: Recent advances in three-dimensional graphene based materials for catalysis applications. Chem. Soc. Rev. 47(6), 2165–2216 (2018)
58. He, Y., et al.: Freestanding three-dimensional graphene/MnO_2 composite networks as ultralight and flexible supercapacitor electrodes. ACS Nano. 7(1), 174–182 (2013)
59. Lee, J.-S., et al.: Three-dimensional nano-foam of few-layer graphene grown by CVD for DSSC. Phys. Chem. Chem. Phys. 14(22), 7938–7943 (2012)
60. Cao, X., Yin, Z., Zhang, H.: Three-dimensional graphene materials: preparation, structures and application in supercapacitors. Energy Environ. Sci. 7(6), 1850–1865 (2014)
61. Zhan, H., et al.: Direct fabrication of 3D graphene on nanoporous anodic alumina by plasma-enhanced chemical vapour deposition. Sci Rep. 6(1), 19822 (2016)
62. Wang, C., et al.: Hierarchical composite electrodes of nickel oxide nanoflake 3D graphene for high-performance pseudocapacitors. Adv. Funct. Mater. 24(40), 6372–6380 (2014)
63. Wang, L., et al.: Three-dimensional Ni(OH)2 nanoflakes/graphene/nickel foam electrode with high rate capability for supercapacitor applications. Int. J. Hydrogen Energy. 39(15), 7876–7884 (2014)
64. Zhou, J., et al.: Free-standing S, N co-doped graphene/Ni foam as highly efficient and stable electrocatalyst for oxygen evolution reaction. Electrochim. Acta. 317, 408–415 (2019)
65. Xu, Y., et al.: Self-assembled graphene hydrogel via a one-step hydrothermal process. ACS Nano. 4(7), 4324–4330 (2010)
66. Wang, Y., et al.: Reduced graphene oxide film with record-high conductivity and mobility. Mater. Today. 21(2), 186–192 (2018)
67. Zhang, W., et al.: Synthesis of Ag/RGO composite as effective conductive ink filler for flexible inkjet printing electronics. Colloid Surf. Physicochem. Eng. Aspect. 490, 232–240 (2016)
68. Cai, Z.-x., et al.: Electrodeposition-assisted synthesis of Ni2P nanosheets on 3D graphene/Ni foam electrode and its performance for electrocatalytic hydrogen production. ChemElectroChem. 2(11), 1665–1671 (2015)
69. Serrano, M.C., et al.: 3D free-standing porous scaffolds made of graphene oxide as substrates for neural cell growth. J Mater. Chem. B. 2(34), 5698–5706 (2014)
70. He, Z., et al.: Architecture engineering of hierarchically porous chitosan/vacuum-stripped graphene scaffold as Bioanode for high performance microbial fuel cell. Nano. Lett. 12(9), 4738–4741 (2012)
71. Jiang, Z., Pei, B., Manthiram, A.: Randomly stacked holey graphene anodes for lithium ion batteries with enhanced electrochemical performance. J. Mater. Chem. 1(26), 7775–7781 (2013)
72. Kong, W., et al.: Holey graphene hydrogel with in-plane pores for high-performance capacitive desalination. Nano. Res. 9(8), 2458–2466 (2016)
73. Jiang, Z., et al.: High performance of a free-standing sulfonic acid functionalised holey graphene oxide paper as a proton conducting polymer electrolyte for air-breathing direct methanol fuel cells. J. Mater. Chem. 2(18), 6494–6503 (2014)
74. Guerrero-Avilés, R., Orellana, W.: Hydrogen storage on cation-decorated biphenylene carbon and nitrogenated holey graphene. Int. J. Hydrogen Energy. 43(51), 22966–22975 (2018)
75. Lee, J.-S., et al.: Metal–air batteries with high energy density: Li–air versus Zn–air. Adv. Energy Mater. 1(1), 34–50 (2011)
76. Park, H.W., et al.: Electrospun porous nanorod perovskite oxide/nitrogen-doped graphene composite as a bi-functional catalyst for metal air batteries. Nano. Energy. 10, 192–200 (2014)
77. Khan, Z., et al.: Hierarchical urchin-shaped α-MnO2 on graphene-coated carbon microfibers: a binder-free electrode for rechargeable aqueous Na–air battery. NPG Asia Mater. 8(7), e294–e294 (2016)

78. Ma, J., et al.: Effects of polystyrene sulfonate/graphene and Mn3O4/graphene on property of aluminium(zinc)-air batteries. Int. J. Hydrogen Energy. 45(23), 13025–13034 (2020)
79. Balandin, A.A.: Thermal properties of graphene and nanostructured carbon materials. Nat. Mater. 10(8), 569–581 (2011)
80. Lee, K.Y., Gupta, M.K., Kim, S.-W.: Transparent flexible stretchable piezoelectric and triboelectric nanogenerators for powering portable electronics. Nano. Energy. 14, 139–160 (2015)
81. Bhunia, R., et al.: Milli-watt power harvesting from dual triboelectric and piezoelectric effects of multifunctional green and robust reduced graphene oxide/P(VDF-TrFE) composite flexible films. ACS Appl. Mater. Interfaces. 11(41), 38177–38189 (2019)
82. Bai, Y., Xu, T., Zhang, X.: Graphene-based biosensors for detection of biomarkers. Micromachines. 11(1), 60 (2020)
83. Luo, H., et al.: Effect of highly dispersed graphene and graphene oxide in 3D nanofibrous bacterial cellulose scaffold on cell responses: a comparative study. Mater. Chem. Phys. 235, 121774 (2019)
84. Song, S., et al.: Biomedical application of graphene: from drug delivery, tumour therapy, to theranostics. Colloids Surf. B Biointerfaces. 185, 110596 (2020)
85. Wang, Y., et al.: Graphene and graphene oxide: biofunctionalisation and applications in biotechnology. Trends Biotechnol. 29(5), 205–212 (2011)
86. Qi, J., et al.: Metal-Catalyst-free carbohydrazide fuel cells with three-dimensional graphene anodes. ChemSusChem. 8(7), 1147–1150 (2015)
87. Cardoso, R.M., et al.: 3D-Printed graphene/polylactic acid electrode for bioanalysis: Biosensing of glucose and simultaneous determination of uric acid and nitrite in biological fluids. Sens. Actuat. B Chem. 307, 127621 (2020)
88. Cheng, X., Wan, Q., Pei, X.: Graphene family materials in bone tissue regeneration: perspectives and challenges. Nanoscale Res. Lett. 13(1), 289 (2018)
89. Cheng, C., et al.: Functional graphene nanomaterials based architectures: biointeractions, fabrications, and emerging biological applications. Chem. Rev. 117(3), 1826–1914 (2017)
90. Chong, Y., et al.: Reduced cytotoxicity of graphene nanosheets mediated by blood-protein coating. ACS Nano. 9(6), 5713–5724 (2015)
91. Peña-Bahamonde, J., et al.: Recent advances in graphene-based biosensor technology with applications in life sciences. J. Nanobiotechnol. 16(1), 75 (2018)
92. Reina, G., et al.: Promises, facts and challenges for graphene in biomedical applications. Chem. Soc. Rev. 46(15), 4400–4416 (2017)

How to cite this article: Thiyagarajan P. A review on three-dimensional graphene: Synthesis, electronic and biotechnology applications-The Unknown Riddles. *IET Nanobiotechnol*. 2021;15:348–357. https://doi.org/10.1049/nbt2.12045